Time resolved amplified FRET identifies protein kinase B activation state as a marker for poor prognosis in clear cell renal cell carcinoma

James Miles[a,e,g], Christopher J. Applebee[a], Pierre Leboucher[b], Sonia Lopez-Fernandez[a], Dae-Jin Lee[c], Rosa Guarch[d], Stephen Ward[e], Peter J. Parker[f], Jose I. López[g,*], Banafshé Larijani[a,*]

---

[a] Cell Biophysics Laboratory, Ikerbasque, Basque Foundation for Science, FASTBASE SOLUTIONS Ltd, Research Centre for Experimental Marine Biology and Biotechnology (PiE) & Biofísika Institute (UPV/EHU, CSIC), University of the Basque Country, Spain

[b] Institut du Cerveau et de la Moelle épinière, Hôpital de la Pitié-Salpêtrière, Paris, France

[c] Basque Center for Applied Mathematics, Bilbao, Bizkaia, Spain

[d] Department of Pathology B, Complejo Hospitalario de Navarra, Pamplona, Spain

[e] Department of Pharmacy and Pharmacology, University of Bath, UK

[f] Protein Phosphorylation Laboratory, The Francis Crick Institute, London, UK and Division of Cancer Studies, King's College London, London, UK

[g] Department of Pathology, Cruces University Hospital, Biocruces Research Institute, University of the Basque Country (UPV/EHU), Barakaldo, Spain

---

Abstract

Purpose: Clear cell Renal Cell Carcinomas (ccRCC), the largest group of renal tumours, are resistant to classical therapies. The determination of the functional state of actionable biomarkers for the assessment of these adenocarcinomas is essential. The dysregulation of the oncoprotein, PKB/Akt has been linked with poor prognoses in human cancers.

Material & methods: We analysed the status of the PKB/Akt pathway in a representative tumour tissue microarray obtained from the primary tumours and their metastases in 60 ccRCC with long term follow up. We sought to define the evolution of this pathway from the primary tumour to the metastatic event and to know the impact of its functional state in tumour aggressiveness and patient survival. Two-site time resolved amplified FRET (A-FRET) was utilised for assessing the activation state of PKB/Akt and this was compared to conventional immunohistochemistry measurements.

Results: Activation state of PKB/Akt in primary tumours defined by A-FRET correlated with poorer overall survival (hazard ratio 0.228; p = 0.002). Whereas, increased protein expression of phosphoPKB/Akt, identified using classical immunohistochemistry, yielded no significant difference (hazard ratio 1.390; p = 0.548). Conclusions: Quantitative determination of PKB/Akt activation in ccRCC primary tumours alongside other diagnostics tools could prove key in taking oncologists closer to an efficient personalised therapy in ccRCC patients.

General significance: The quantitative imaging technology based on Amplified-FRET can rapidly analyse protein activation states and molecular interactions. It could be used for prognosis and assess drug function during the early cycles of chemotherapy. It enables evaluation of clinical efficiency of personalised cancer treatment.

1. Introduction

Clear cell renal cell carcinomas (ccRCCs) are a major health concern in the West as they are quite a common aggressive radio- and chemo- resistant neoplasm [1]. Only surgery has demonstrated a significant impact in patient survival, the 5-year overall mortality of this neoplasm is still reaching around 40% [2]. Truncal mutations in the Von Hippel-Lindau VHL tumour suppressor gene are the hallmark of this pathology, but therapies against this target have elicited, to date, only partial responses. These disappointing results are mainly related to the inherent high intratumoral heterogeneity (ITH) that ccRCCs display to the point that ITH is nowadays a major obstacle to the implementation of efficient therapies impacting significantly on patient survival [3].

The aim of this study is to determine whether the phosphoinositide 3-kinase (PI3K)/protein kinase B (PKB/Akt) dysregulation is implicated in the mechanisms underlying ccRCC carcinogenesis and its hypothe- tical impact on patient survival. To pursue this investigation a recently developed approach was utilised to determine the functional status of the PKB/Akt signalling pathway [4].

Protein kinase B (PKB/Akt) is a kinase from the AGC kinase superfamily which promotes cell growth, survival and proliferation [5,6]. Upon the binding of a growth factor receptor to a receptor tyrosine kinase, phosphatidylinositol 4,5-bisphosphate ($PtdIns(4,5)P_2$) is phosphorylated, by phosphoinositide 3-kinase (PI3K) to phosphatidy- linositol 3,4,5-triphosphate ($PtdIns(3,4,5)P_3$). This transient formation of $PtdIns(3,4,5)P_3$ recruits PKB and phosphoinositide-dependent protein kinase 1 (PDK1) to the plasma membrane. Upon the change in conformation of PKB, PDK1 phosphorylates threonine-308 to partially active it [7,8]. Full activation is achieved by m-TOR in complex 2 which phosphorylates serine 473 [9]. An overview of the PKB signalling pathway is shown in Fig. 1. PKB is known to be dysregulated in many human cancer [5]. This dysregulation can occur via the loss of inhibition through phosphatase and tensin homolog (PTEN) for example, or through the upregulation of the PI3K-Akt pathway [6,10,11]. Alternatively, a mutation of PKB itself could cause dysregulation within this pathway [12].

Currently, the use of fluorescent microscopy to detect protein ex- pression is based on measuring the intensity and therefore proves to be imprecise; as well as lacking a dynamic range for providing a detailed view on the activation state of oncoproteins in the diagnosis and prognosis of various cancers. Assessing the expression levels of proteins does not provide information on the activation states of the protein in the advancement of a cancer. This is important as expression levels and activation states of oncoproteins do not necessarily correlate [4,13]. Our method uses amplified Förster Resonance Energy Transfer (FRET), detected by a multiple frequency domain fluorescent lifetime imaging microscopy (mf FLIM), to assess the activation of different oncoproteins in primary and metastatic tumours of the same patients. It has been previously shown that this method, when used to assess PKB activation in breast tumours, correlated a higher PKB activation with a worse prognosis [4].

The principles of FRET involve the non-radiative transfer of energy from one chromophore to another via dipoledipole interactions at a distance equal to or < 10 nm. An appropriately selected donor chromophore must have an emission spectrum that overlaps with the ex- citation spectrum of the chosen acceptor chromophore. When excited in the presence of an acceptor, the lifetime of a donor is decreased due to the depopulation of its excited state, where its energy is non-radiatively transferred to the acceptor chromophore [14]. The fluorescent labelling of PKB on both serine and threonine sites will experience FRET upon the increase in the activation state of PKB/Akt.

Exploiting this quantitative methodology has enabled us to show that the PKB/Akt activation in ccRCC primary tumours alongside other diagnostics tools could prove key in taking oncologists closer to an efficient personalised therapy in ccRCC patients.

2. Materials and methods

The authors declare that all the experiments carried out in this study comply with current Spanish and European Union legal regulations. Samples and data from patients included in this study were obtained from the medical records and archives of the Pathology Lab (Cruces University Hospital). All patients were informed about the potential use for research of their surgically resected tissues, and accepted this

eventuality by signing a specific document. This study was approved by the Ethical and Scientific Committee (CEIC-Euskadi PI2015060).

2.1. Patient samples

Two experienced uropathologists (RG, JIL) performed the pathological analysis, re-assigned grade and stage to all tumours and selected the appropriate tumour areas for analysis, including them in tumour microarrays (TMAs). The International Society of Urological Pathology (ISUP) 2013 tumour grading system [15] was assigned to every sample in the TMA on routine haematoxylin and eosin sections. Grade was grouped as low (G1/2) and high (G3/4) for higher consistency. UICC 2010 tumour staging system [16] was assigned to every

case at the time of pathological diagnoses on nephrectomy specimens. Staging was grouped as pT1/2 (tumours confined to the kidney) and pT3 (tumours invading outside the kidney).

2.2. TMA preparation

In every case, well preserved tumour areas of the highest grade, both in the primary tumour and its metastasis, were selected for analysis. Samples of 2.5 mm in diameter of these areas were obtained from the paraffin blocks and placed randomly in TMAs in a routine way to ensure a blind evaluation. Internal controls were included in all TMAs. Unstained 4 µm-thick samples of TMAs were mounted on slides ready for FRET analysis.

2.3. Antibodies and reagents

Monoclonal antibodies, rabbit anti-pAkt and mouse anti-panAkt were purchased from Cell Signalling Technology. Pierce endogenous peroxidase suppressor was also obtained from Thermo Fisher Scientific (catalogue no. 35000). AffiniPure F(ab′)$_2$ fragment donkey anti-rabbit IgG and peroxidase-conjugated AffiniPure F(ab′)$_2$ fragment donkey anti-rabbit IgG were purchased from Jackson Immuno Research Laboratories. ATTO 488 NHS ester was purchased and was conjugated to the AffiniPure F(ab′)$_2$ IgG as described in [4]. Prolong diamond anti-fade mount (catalogue no. P36970), bovine serum albumin (BSA) blocking reagent, amplification buffer and tyramide were all obtained from Life Technologies (catalogue nos. T20915COMPONENT - D, E and A).

2.4. Förster resonance energy transfer (FRET) by fluorescence lifetime imaging microscopy (FLIM)

2.4.1. Two-site amplified FRET assay for PKB/Akt activation quantification

The slides underwent de-waxing and rehydration followed by heat antigen retrieval in Tris-EDTA (pH 9.0) buffer. Slides were incubated with peroxidase suppressor for 30 min. Afterwards slides were incubated for 1 h with fresh 1% (10 mg/ml) BSA blocking buffer. Following this the slides were incubated overnight at 4 °C with the primary antibodies (pan-Akt 1:50, p-Akt 1:100). For secondary anti- body labelling, donor only slides were incubated with Fab-ATTO488 (1:100) and donor acceptor slides with Fab-ATTO488 (1:100) and Fab-HRP (1:200) for 2 h at room temperature. Tyramide signal amplifica- tion was carried out on donor/acceptor slides. Fab-HRP is bound to the primary acceptor antibodies. Tyramide which is conjugated to Alexa594 is then added which, in the presence of H_2O_2, leads to the binding of the Alexa594 chromophore to the HRP molecule, thus fluorescently labelling the acceptor site. Slides were mounted with Prolong Diamond anti-fade mount.

2.4.2. Analysis of biomarker activation using multiple frequency domain FLIM

Immunohistochemistry (IHC) and immunofluorescence (IF) both operate around a one-site assay whereas A-FRET employs the use of a two-site assay. A one-site assay detects only one antigen site at a time and induces non-specificity. A two-site assay detects two antigen sites simultaneously hence rendering an augmented precision. The conjugation of the

chromophores to Fab fragments, which bind to the two primary antibodies, allowed the critical FRET distance of 10 nm or less to be kept and provided a suitable tool for measuring the activation state of a given biomarker. To detect the signal of a sample with good precision and overcome autofluorescence, especially in fixed tissue samples, a signal to noise ratio of at least 4-fold must be observed. To achieve this, tyramide signal amplification was carried out.

Using a high throughput mfFLIM (FASTBASE SOLUTIONS Ltd. and Lambert Instruments), a mapping file was created semi-automatically which mapped each tumour core according to its position on the slide. Mapping the whole tumour core allowed each sample to be analysed completely rather than using segmental analysis. Images and results were automatically acquired from the arrays according to their positioning. Phase, lifetimes and average intensities were all calculated automatically and saved as an excel file, as well as lifetime images.

2.5. Statistical analysis

Statistical analysis was performed using the GraphPad Prism software to create Kaplan-Meier survival curves and Origin Pro8 used to provide statistical analysis and generate box and whisker plots. Statistical differences were calculated between groups using the Mann-Whitney U test (values indicated within the box and whisker plots). The Mann-Whitney U test is a nonparametric test which does not assume a normal distribution of results. P values $\leqslant 0.05$ indicated a statistical difference from the null hypothesis. Box and whisker plots represent the 25–75% range (box) and the 1–99 range (whiskers). Statistical differences are indicated with p values $\leqslant 0.05$. For Kaplan-Meier survival curves, overall survival was plotted, which calculated a patient's time from diagnosis until death or until the patient was last seen. The hazard ratio was also calculated for each Kaplan-Meier curve. Multivariate analysis was also performed to exclude influences among the evaluated parameters. A non-parametric Mann-Whitney U test was also used to see if there was correlation between different parameters and FRET efficiency or intensity and plotted as a Mann-Whitney plot.

3. Results

3.1. Patient data

The series includes 60 patients diagnosed, treated and followed in the Cruces University Hospital from 1990 to 2014. Males predominated in the series (46 M/14F) with an average age of 58.5 years (range 25–83). Primary tumours were located in the right kidney in 29 cases and in the left kidney in 31 cases. The average tumour diameter was 8.5 cm (range 2–19). Thirty-two primary tumours were organ confined (pT1 and pT2) at the time of diagnosis. Twenty-five cases were low grade tumours (grades G1/2) and 35 were high grade (grades G3/4). At the time when the follow-up was closed (Dec 2015), 40 (66.6%) patients had died of disease. The average clinical follow up was 67.5 months (range 1–240). The elapsed time between the diagnosis of the primary tumour and the metastasis widely oscillated, from 0 to 204 months. Epithelial organs, mostly lung and pancreas, were the

sites of the metastatic seed in 29 cases (48.3%), lymph nodes in 13 cases (21.6%) and soft tissues/bone in 18 cases (30%).

Fig. 2A shows haematoxylin and eosin staining's for typical low (left hand panel) and high (right hand panel) grade ccRCC samples. ISUP grading system [7] was assigned to every sample in the TMA. Samples were grouped as low (G1/2) and high (G3/4) grades for higher con- sistency. Fig. 2B shows fluorescent intensity maps and lifetime maps for the primary (left hand panel) and metastatic (right hand panel) tumour samples of one patient. The two-site assay was used to label pan Akt and pThr308-Akt simultaneously for each patient sample. The donor and acceptor intensity images indicate PKB/Akt and pThr308-Akt expres- sion levels respectively. These images were equivalent to IHC images where little difference was observed between the primary and meta- static samples. Conversely, in the lifetime maps, a clear difference was observed between the samples, where lower lifetimes (see pseudo- colour scale) were indicative of higher PKB/Akt activation state. Some difference in fluorescence lifetime can be observed between the donor only samples of the primary and metastatic tumours of each patient however comparisons should be made between the donor and donor/ acceptor of the same patient. Fig. 2C shows the primary and metastatic PKB/Akt activation state for all patients determined by A-FRET. Some patients, such as patient 56, had a negligible PKB/Akt activation state in the primary tumour FRET Efficiency (Ef) = 0%. However, the FRET efficiency increased to 44.2% in the equivalent metastatic tumour. Thus, a low activation state of PKB/Akt did not necessarily correlate with an equivalent activation state in its corresponding metastatic evolution. Fig. 2D shows the Ef of different patients plotted as Box and Whiskers distributions. The median Ef differences between primary and metastatic tumour samples were compared to noncancerous renal control tissue. The non-parametric Mann-Witney U statistical tests illustrate a significant difference between the median of the Box and Whiskers plots of primary and metastatic tumours ($p = 3.81 \times 10^{-5}$) and between metastatic and noncancerous control tissue ($p = 3.83 \times 10^{-7}$). The Ef parameter was utilised as a variable to assess patient prognosis. The highest 25% and lowest 75% Ef values were used to plot the Kaplan-Meier survival curves. Fig. 3A shows that PKB/ Akt activation state correlated with a poorer clinical outcome. The patients with the highest 25% of PKB/Akt activation were shown to have poorer prognoses when compared to the lower 75% (n = 16, p = 0.0018, HR = 0.22279 with 95% CI, 0.052–1.005). When using intensity and protein expression as a method of analysis, a significant difference was not observed between the groups (n = 16, p = 0.5483, HR = 1.3912 with 95% CI, 0.484–4.000). Fig. 3B and C summarise Mann-Whitney U tests performed on the primary ccRCC tumours. These statistical analyses determined the correlations between Ef or IHC methods (pThr308-Akt-acceptor intensity) with histological grading (low (G1/2) and high (G3/4) grades) and staging (pT1/2 or pT3 in primary tumours). Neither A-FRET nor intensity determinations showed significant correlations with tumour grading or staging (con- fined versus not confined).

4. Discussion

PKB/Akt is an oncoprotein, which is dysregulated in many human cancers [5]. Recently we have shown that its activation state is correlated to poor prognosis in breast cancer patients

[4]. We also demonstrated that expression levels and activation states of oncoproteins did not necessarily correlate [4]. We therefore sought to assess whether in ccRCC patients, where the tyrosine kinase receptor pathways are dysregulated, PKB/Akt activation states would identify a worse clinical outcome. To validate this assessment, we constructed formalin-fixed paraffin embedded (FFPE) TMAs that included representative samples both of primary tumours and their metastases, either synchronic or metachronic, of 60 ccRCC patients with long-term clinical follow-up. A two-site time resolved amplified FRET method, detected by high throughput mfFLIM, was exploited to assess the functional state of PKB/ Akt in these patients. Ef was utilised for determining the activation state of PKB/Akt [4]. Some differences in fluorescence lifetime occurred between donor only samples when comparing primary and metastatic samples; this is due to changes in the microenvironment between different tumours, such as pH and tissue type as metastatic tumours have the capability of creating a new tumour microenvironment in a range of tissue types. Comparisons between fluorescence lifetimes are made between donor and donor/acceptor samples of the same patient as these are tissues of the same type and from the same tumour microenviron- ment.

In summary, we have shown for the first time that the activation state of PKB/Akt in ccRCC patients, measured by A-FRET (but not by IHC intensity) was correlated with poorer overall survival. This assay is able to directly monitor the activation state of PKB/Akt in primary and metastatic ccRCC tissue, and could be used to monitor posttranslational modifications and complexes of other oncoproteins. The ability to ac- curately quantify the functional state of oncoproteins has important implications as a high number of ccRCCs, within their evolution, de- velop distant lymphatic and/or haematogenous metastases [17], whereby the prognostic impact of classical histologic features in the primary tumour diminishes or disappears. Here prognostic models turn to the prediction of response to systemic therapy [18]. Therefore, in such a context, companion diagnostics such as A-FRET will prove valuable.

Acknowledgements

We thank the Technical staff at the Pathology Unit at Cruces Hospital for their support and help with sample TMA preparations. Fig. 1 was adapted from the thesis of Madeline Parker.

Competing interests

PL, PJP and BL are co-founders of FASTBASE Solutions, which uses A-FRET to develop insights into human disease.

Author contributions

JM, JIL and BL. designed the experiments; JM, SW, PJP, JIL and BL. wrote the manuscript; JM, SL and CA performed the experiments; JM, CA and BL analysed the data; PL set up automated algorithm; RG, JIL made the histological evaluation and selected tumour areas for the TMAs, DJL performed the statistical analysis; all authors reviewed and approved the manuscript prior to submission.

Funding

We also acknowledge the support of the Ikerbasque Foundation of Science; the Spanish Ministry of Economy for the grants [grant number BFU 2011-28566] to B.L.; Basque Government through the BERC 360 2014–2017; the Spanish Ministry of Economy and Competitiveness MINECO and FEDER: BCAM Severo Ochoa excellence accreditation SEV-2013-0323 to DJL.

References

. [1] R.L. Siegel, K.D. Miller, A. Jemal, Cancer statistics, 2016, CA Cancer J. Clin. 66 (1) (2016) 7–30.

. [2] F. Audenet, et al., Genetic pathways involved in carcinogenesis of clear cell renal cell carcinoma: genomics towards personalized medicine, BJU Int. 109 (12) (2012) 1864–1870.

. [3] C. Hiley, et al., Deciphering intratumor heterogeneity and temporal acquisition of driver events to refine precision medicine, Genome Biol. 15 (8) (2014) 453.

. [4] S. Veeriah, et al., High-throughput time-resolved FRET reveals Akt/PKB activation as a poor prognostic marker in breast cancer, Cancer Res. 74 (18) (2014) 4983–4995.

. [5] A. Bellacosa, et al., Activation of AKT kinases in cancer: implications for therapeutic targeting, Adv. Cancer Res. 94 (2005) 29–86.

. [6] D.D. Sarbassov, et al., Phosphorylation and regulation of Akt/PKB by the rictor-mTOR complex, Science 307 (5712) (2005) 1098–1101.

. [7] V. Calleja, et al., Intramolecular and intermolecular interactions of protein kinase B define its activation in vivo, PLoS Biol. 5 (4) (2007) e95.

. [8] V. Calleja, et al., Role of a novel PH-kinase domain interface in PKB/Akt regulation: structural mechanism for allosteric inhibition, PLoS Biol. 7 (1) (2009) e17.

. [9] J. Feng, et al., Identification of a PKB/Akt hydrophobic motif Ser-473 kinase as DNA-dependent protein kinase, J. Biol. Chem. 279 (39) (2004) 41189–41196.

. [10] L.C. Cantley, B.G. Neel, New insights into tumor suppression: PTEN suppresses tumor formation by restraining the phosphoinositide 3-kinase/AKT pathway, Proc. Natl. Acad. Sci. U. S. A. 96 (8) (1999) 4240–4245.

. [11] K. Stemke-Hale, et al., An integrative genomic and proteomic analysis of PIK3CA, PTEN, and AKT mutations in breast cancer, Cancer Res. 68 (15) (2008) 6084–6091.

. [12] J.D. Carpten, et al., A transforming mutation in the pleckstrin homology domain of AKT1 in cancer, Nature 448 (7152) (2007) 439–444.

. [13] A. Kong, et al., Prognostic value of an activation state marker for epidermal growth factor receptor in tissue microarrays of head and neck cancer, Cancer Res. 66 (5) (2006) 2834–2843.

. [14] B. Valeur, Molecular Fluorescence: Principles and Applications, xiv Wiley-VCH, Weinheim; Chichester, 2002 (387 p.).

. [15] B. Delahunt, et al., The International Society of Urological Pathology (ISUP) grading system for renal cell carcinoma and other prognostic parameters, Am. J. Surg. Pathol. 37 (10) (2013) 1490–1504.

. [16] S.B. Edge, C.C. Compton, The American Joint Committee on Cancer: the 7th edition of the AJCC cancer staging manual and the future of TNM, Ann. Surg. Oncol. 17 (6) (2010) 1471–1474.

. [17] H.L. Kim, et al., Using protein expressions to predict survival in clear cell renal carcinoma, Clin. Cancer Res. 10 (16) (2004) 5464–5471.

. [18] A. Volpe, J.J. Patard, Prognostic factors in renal cell carcinoma, World J. Urol. 28 (3) (2010) 319–327.

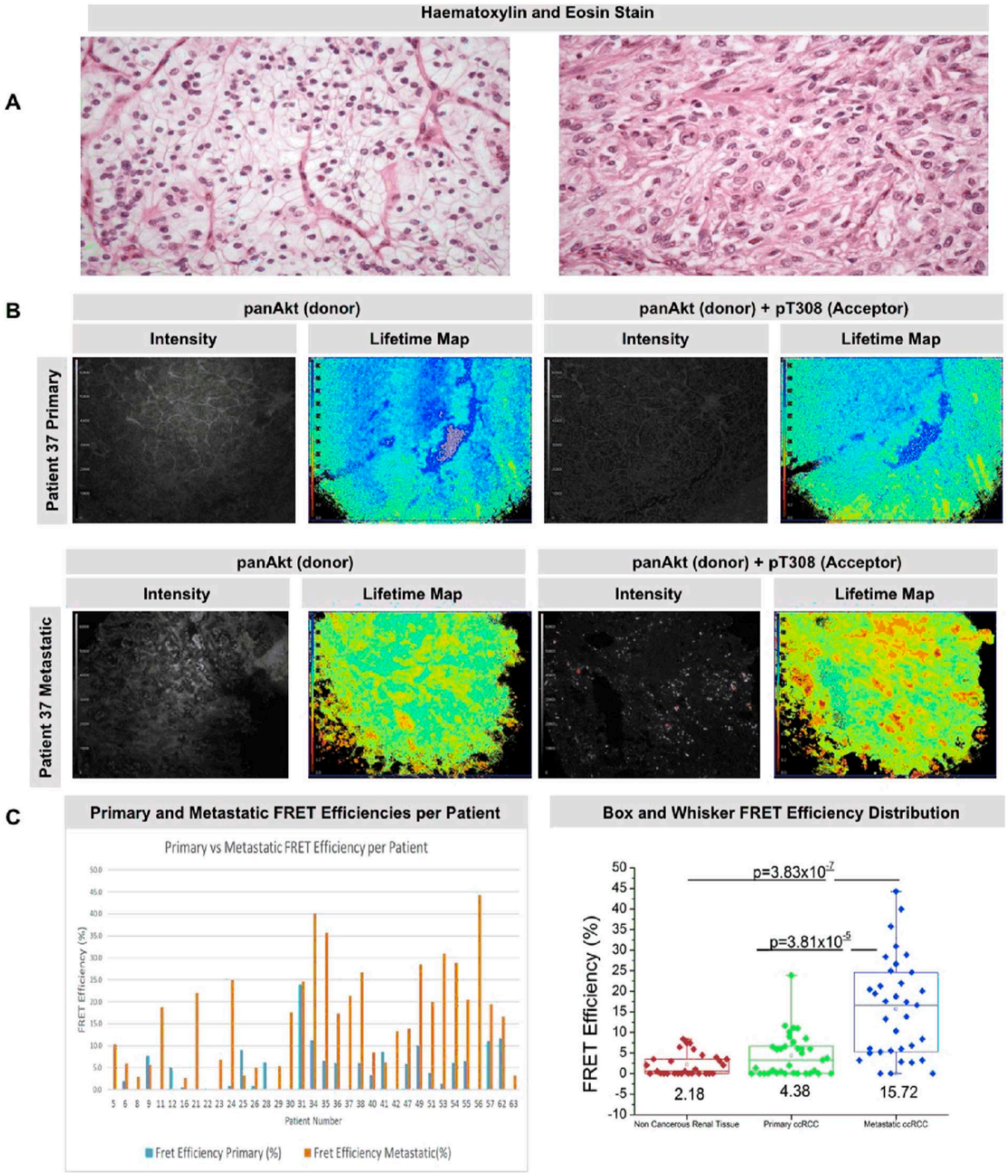

Fig. 2. PKB/Akt activation is higher in metastatic ccRCC tumours in FFPE TMAs. A, Low-(left) and high-(right) grade ccRCCs B, the intensity images (corresponding to protein expression levels) of PKB/Akt and pAkt expression levels do not yield differences. Lifetime maps however do yield significant differences between primary and metastatic ccRCC samples. C, PKB/Akt activation state determined by A-FRET from primary to metastatic tumours for each patient. Patients 9 and 31 have higher Akt activation in their primary tumours D, the Box and Whisker plots show an increase in PKB/Akt activation from the non-tumour control tissue to the primary ccRCC cores with a significant difference of ($p = 3.81 \times 10^{-5}$). Each point on the Box and Whisker plot indicates the activation state of the primary and metastatic tumours of each patient. A larger increase in activation is shown from primary cores to metastatic cores. P values are shown between significantly different groups.

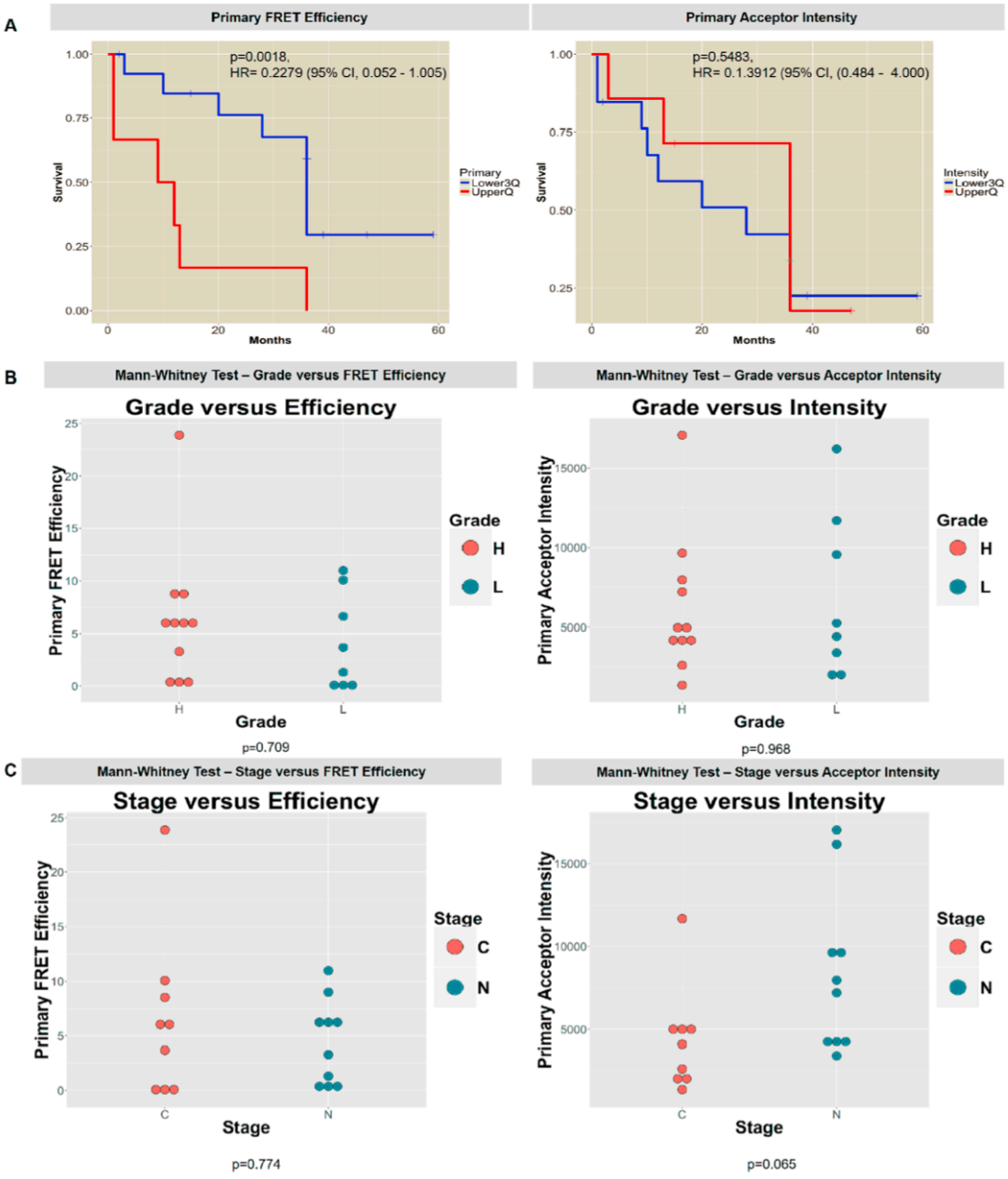

Fig. 3. PKB/Akt activation state correlates with poor overall survival in ccRCC. A, shows the survival outcomes related to PKB/Akt activation as determined by A-FRET (left panel) or by conventional IHC (right panel). A highly significant difference was observed between the upper quartile of FRET Efficiency and the lower 3 quartiles FRET Efficiency. No difference was detected when survival is determined by IHC intensity of the activation state of PKB/Akt. B, Both A-FRET and IHC detections did not relate to grading (High H and Low L) p = 0.709 and p = 0.968. C, A-FRET and IHC measurements did not show significant correlations between staging (confined, c, versus non-confined, n, primary tumours) p = 0.774 and p = 0.065 respectively.